AIRSPEED CALIBRATION SERVICE

NIST Special Publication 250-79

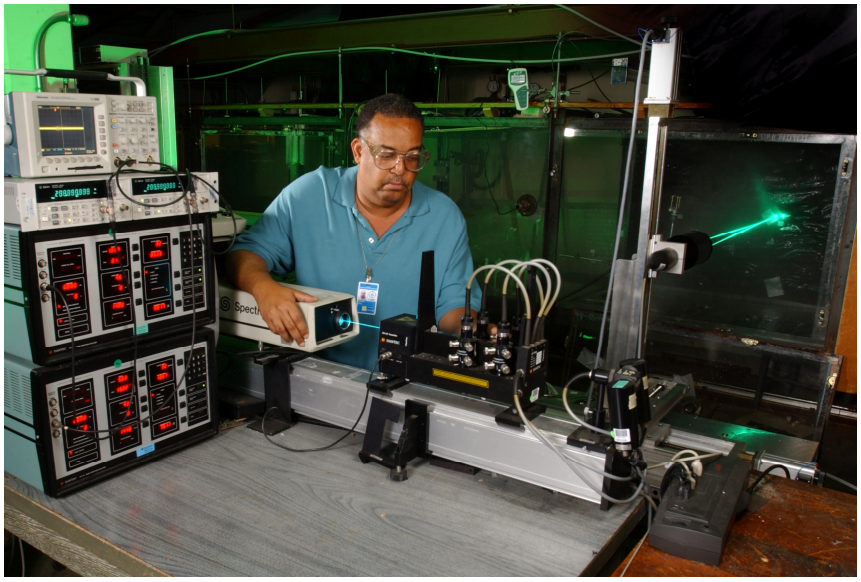

T.T. Yeh and J. M. Hall

Fluid Metrology Group
Process Measurements Division
Chemical Science and Technology Laboratory
National Institute of Standards and Technology
Gaithersburg, MD 20899

Certain commercial equipment, instruments, or materials are identified in this paper to foster understanding. Such identification does not imply recommendation or endorsement by the National Institute of Standards and Technology, nor does it imply that the materials or equipment identified are necessarily the best available for the purpose

Table of Contents **Page**

Abstract

The National Institute of Standards and Technology (NIST) provides calibration services for airspeed instrumentation such as Pitot-static tubes, anemometers (ultrasonic, thermal or hot-wire, cup, and propeller types) as well as others. The NIST calibration system consists of a wind tunnel and a Laser Doppler Anemometer (LDA). The standard for airspeed measurement is a fiber optic LDA, which is calibrated with known velocities produced by a rotating disk. A Pitot-static tube probe and thermal anemometer are used as check standards. The wind tunnel used for the calibration has a test cross section of 1.5 m by 2.1 m and water droplets injected into the wind tunnel from fine spray nozzles provide the light scattering particles necessary for the operation of the LDA. The range of the airspeed in the calibration service is from 0.15 m/s to 40 m/s.

This document also describes the methods of operation and uncertainty of NIST airspeed standards. An extensive component analysis of the system was performed. Over the calibration range, the airspeed uncertainty is found to be a function of airspeed and the expanded uncertainty at 95 % confidence level, i.e. $k = 2$, in m/s can be expressed by the root-sum-square of $0.0064V$ and 0.0036 m/s, where V is airspeed in m/s. This gives a maximum uncertainty of 2.5 % (0.0038 m/s) at the lowest airspeed of 0.15 m/s and a minimum uncertainty of 0.65 % (0.26 m/s) at the highest speed of 40 m/s.

1. Introduction

The National Institute of Standards and Technology (NIST) provides calibration services for airspeed instrumentation such as Pitot-static tubes, anemometers (hot-wire, cup, and propeller types) as well as others. These calibration services provide traceability with a calibration report that documents the calibration procedure, the calibration results, and their uncertainties for airspeed sensor manufacturers, secondary airspeed calibration laboratories, and sensor users. The customer may use the sensor and its calibration results in different ways. It is often used as a transfer standard to compare the customer's primary standards to the NIST primary standards so that the customer can establish traceability, validate their uncertainty analysis, and demonstrate proficiency. Customers with no primary standards use their NIST calibrated airspeed sensors as working standards or reference standards in their laboratory to calibrate other airspeed sensors.

NIST's airspeed calibration system consists of a dual test section wind tunnel and a LDA airspeed measurement system. The airspeed is measured with a Dantec LDA. A Pitot-static tube probe and thermal anemometer are used as check standards during every calibration. Routine calibrations are done by direct comparison of the averaged response of the instrument under test (IUT) with the response of the NIST LDA standard in the same air stream.

2. Description of the Measurement Service

Customers should consult the web address www.cstl.nist.gov/div836/Fluid Metrology Group to find the most current information regarding our calibration services, calibration fees, technical contacts, and flowmeter submittal procedures.

NIST provides calibration services for various air speed instrumentations. The calibration facility is a dual section wind tunnel, which has two interchangeable test sections, together, spans a velocity range of 0.15 m/s to 67 m/s (0.34 mph to 150 mph). Currently, NIST provides air speed calibration services over a range of 0.15 m/s to 40 m/s. NIST is working to incorporate additional setups so that the air speed calibration service will reach 67 m/s. Routine calibrations are done by direct comparison of the response of the instrument under test (IUT) with the response of a NIST standard instrument in the same air stream. Airspeed is measured with a calibrated Dantec laser Doppler anemometer (LDA). A Pitot tubes and a thermal anemometer are used as the check standards. The expanded uncertainties for the airspeed standard, in m/s as a function of air speed, is given as $k\sqrt{(0.0032\,V_{LDA})^2 + (0.0018\,)^2}$ with a coverage factor of $k = 2$ where V_{LDA} is the indicated airspeed from the LDA in the unit of m/s. It varies from 2.5 % at the lowest speed of 0.15 m/s to 0.65 % to the highest speed of 40 m/s.

The temperature, pressure, and the relative humidity in the airflow are also measured in the test section of the wind tunnel during the test. A normal airspeed calibration performed by the NIST Fluid Metrology Group consists of several speeds spread over the range of the given airspeed sensor. Two calibration cycles are done separated by a shutdown. In each calibration cycle, the air speed is measured five times at each airspeed set point. Therefore, the final data set consists of ten speed measurements made at each speed set point. The sets of five measurements can be used to assess repeatability, while the sets of ten can be used to assess reproducibility. For further explanation, see the sample calibration report in the Appendix A of this document. Variations on the number of speed set points, spacing of the set points, and the number of repeated measurements can be discussed with the NIST technical contacts. However, for data quality assurance reasons, we rarely will conduct calibrations involving fewer than five speed set points and two sets of three speed measurements at each set point. The Fluid Metrology Group prefers to present airspeed calibration results in a dimensionless format based on the speed ratio.

3. Procedures for Submitting an Airspeed sensor for Calibration

The Fluid Metrology Group follows the policies and procedures described in Chapters 1, 2, and 3 of the NIST Calibration Services Users Guide [1]. These chapters can be found on the internet at the following addresses:
http://ts.nist.gov/measurementServices/Calibrations/policy.cfm,
http://ts.nist.gov/measurementServices/Calibrations/domestic.cfm, and
http://ts.nist.gov/measurementServices/Calibrations/foreign.cfm

Chapter 2 gives instructions for ordering a calibration for domestic customers and has the sub-headings: A.) Customer Inquiries, B.) Pre-arrangements and Scheduling, C.) Purchase

Orders, D.) Shipping, Insurance, and Risk of Loss, E.) Turnaround Time, and F.) Customer Checklist. Chapter 3 gives special instructions for customers outside the United States. The web address www.cstl.nist.gov/div836/Fluid Metrology Group has information more specific to the airspeed calibration service, including the technical contacts in the Fluid Metrology Group, fee estimates, and turn around times.

4. Airspeed Calibration Facilities

NIST airspeed calibrations are done in a dual section wind tunnel [2] as shown in Fig. 1. The tunnel is a closed-circuit facility lying in a horizontal plane and has two interchangeable test sections. These two test section ducts ride "piggy back" on a cable hoisting arrangement. The upper test section is 12 m long and has a system of parallel arms along the sides which allow the side walls to be adjusted. The width of the test section is variable; however, the normal dimensions are 2.1 m high and 1.5 m wide. The top speed in the upper test section is 45 m/s. In the lower test section, the 2.1 m height at the entrance is gradually reduced in the flow direction to 1.2 m forming a venturi-like duct so that the top speed is 67 m/s. The effective working length is 3.0 m within the overall 12 m length. All sides of the lower test section are fixed. Currently the airspeed calibrations are done only in the upper test section over a range of 0.15 m/s to 40 m/s. NIST is working to incorporate additional setups (e.g. a better seeding conditions) so that the airspeed calibration service will reach 67 m/s.

The downstream end of the test sections is vented to the room establishing this point in the circuit as being near atmospheric pressure. From the test section, the flow passes into a 5º diffuser, around two 90º bends containing turning vanes and into the drive section which measures 3.8 m by 4.4 m at the location of a cooling coil used to stabilize the tunnel temperature. The cooling coil is situated between the drive motor and the fan so that the fan drive shaft passes through the center of the coil. A rectangular-to-round transition section makes the connection to the drive fan inlet. The entire drive mechanism, along with the cooling coil, is mounted on a large concrete slab, which is isolated from the building floor with springs to minimize the transmission of vibration. The main tunnel duct is attached to the drive section at each end by means of flexible boots.

The fan is powered by a variable speed 300 kW direct current (DC) motor. The DC voltage is supplied by a 370 kW motor-generator set. The maximum fan speed is 600 revolutions per minute and is controlled by a feedback loop producing shaft revolutions stable to within ±0.1%. The fan is 2.4 m in diameter with two axial stages and manually adjustable-pitch blades. Downstream of the fan the flow passes through a circular-to-square transition section and into a five-degree diffuser followed by the two more special diffusers sets. The upstream diffuser consists of two sets of turning vanes, a 1 cm by 7.6 cm honeycomb, and the downstream wide-angle diffuser containing 6 screens. After the diffuser, there is a 6.1 m by 7.5 m settling chamber having 9 screens. From the settling chamber the airflow passes through an entrance cone and into the 1.5 m by 2.1 m test section.

The combined effects of the honeycomb, screens, and a contraction ratio of 14.5:1 provide test section longitudinal free-stream turbulence levels of 0.07 % over most of the speed range and

a transverse velocity gradient less than 1 % within a "working window" of 90 % of the test-section areas.

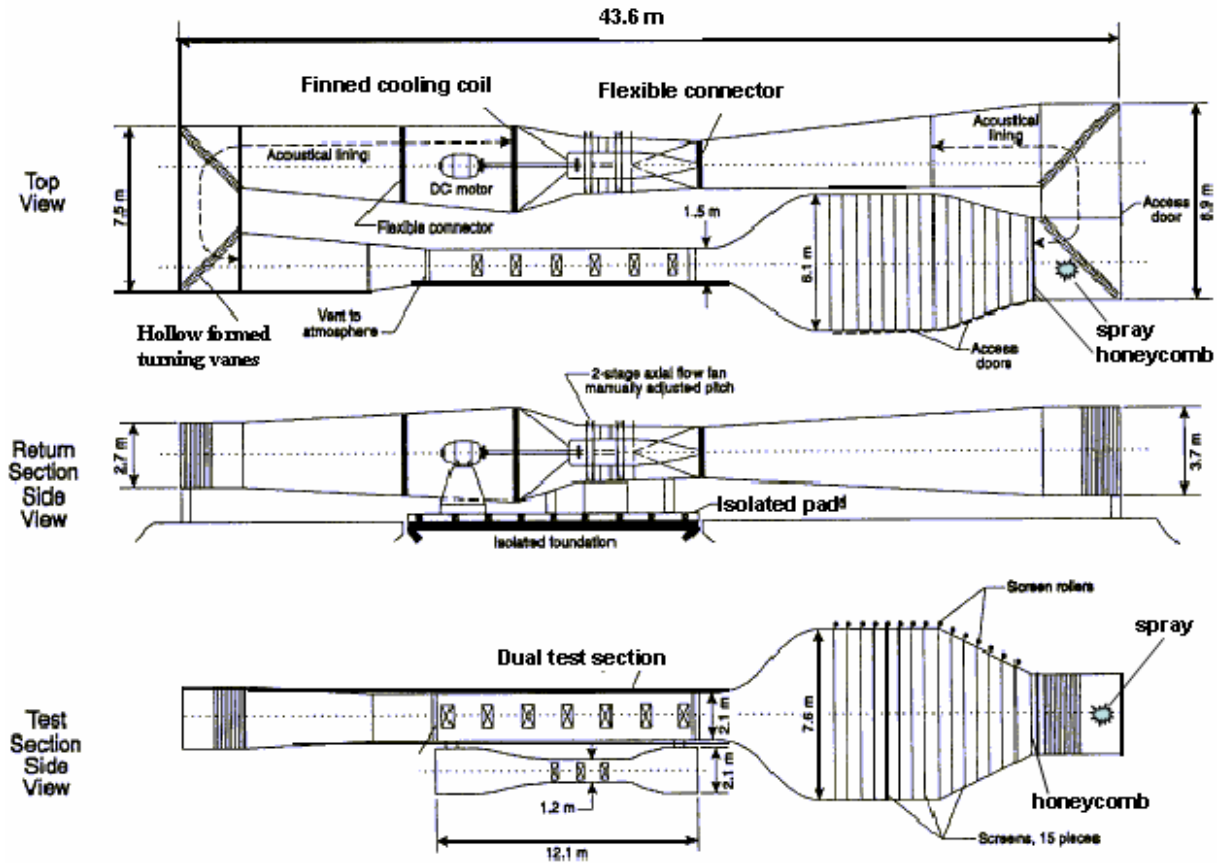

Figure 1 NIST Wind Tunnel for Airspeed Calibration Service.

To provide the light scattering particles necessary for the operation of the LDA, water droplets, produced by several fine air-water spray nozzles, are introduced into the tunnel before the wide-angle diffuser and directed toward the honeycomb (see Fig. 1 for the nozzle location). Fig. 2 shows the fine water droplets with the spray nozzles. The spray can be adjusted to optimize the data rate for the LDA signal processor.

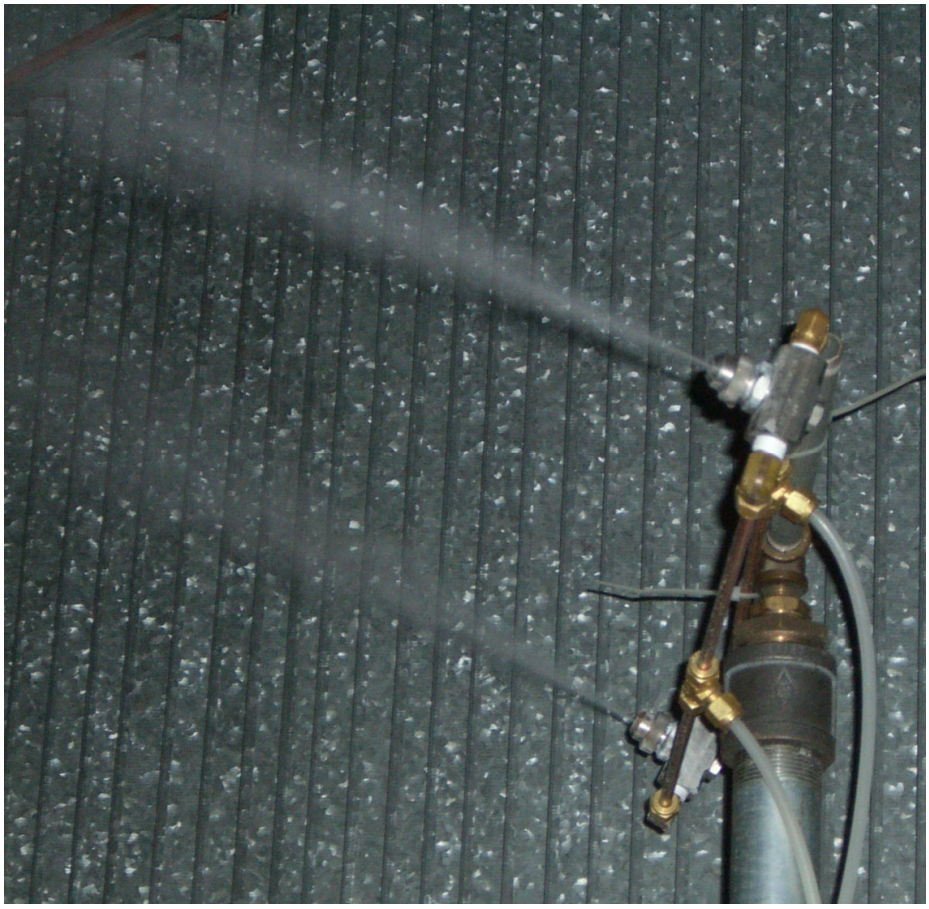

Figure 2 Photo of fine water droplets with the air-water spray nozzles

5. Primary Airspeed Standard -- LDA

The primary standard for airspeed measurement at NIST is a fiber optic LDA. This instrument has been characterized by calibrating its indicated speed using particles of known speed as discussed below.

5.1 Operation Principle of Laser Doppler Anemometry

An LDA measures the velocity of a particle moving in a plane perpendicular to the bisecting plane of the two converging laser beams [3, 4]. The laser velocimetry operated in a differential mode is commonly used to generate the Doppler frequency of the scattered light and used to measure the particle/fluid speed. The NIST LDA is a differential laser velocimetry system. It splits a laser beam into two beams in a plane and then recombines them at a small intersection angle by using a transmitting focus lens. In the intersection volume, the two beams are mutually coherent, collimated of like polarization and of equal intensity. The interaction between these two laser beams results in a three-dimensional region (sensing volume) which contains an

interference pattern that is composed of parallel light and dark fringes. Small particles, entrained in, and moving at the same speed as the air stream, scatter light as they pass through each bright fringe in the intersection volume. The NIST LDA operates in a backscattering configuration. Scattered light from the particle moving through the fringe pattern is collected by the same lens used to transmit the two laser beams and focused onto a fiber detector. Because of the periodic fringe pattern, the scattered light will be intensity modulated at a frequency proportional to the component of the particle velocity perpendicular to the fringe pattern. The correct airspeed is measured when the probe is properly aligned such that the bisecting plane of the two laser beams is perpendicular to the direction of the flow.

The spacing between the bright fringes, d depends on the angle θ between the two laser beams and the laser wavelength λ as

$$d = \frac{\lambda}{2\sin\left(\frac{\theta}{2}\right)} \tag{1}$$

As shown in Fig. 3, when two parallel beams having a separation of *h* are combined by a lens having a focal length of f_L, the beams intersect at the angle

$$\theta = 2\tan^{-1}\left(\frac{h}{2f_L}\right) \tag{2}$$

In the context of airspeed measurement, the spacing d between the bright fringes serves as the length scale.

To resolve the sign of the velocity, a frequency offset generated by a Bragg cell is used to move the fringe pattern through the measuring volume and across the scattering particle. Fiber optic cables transmit laser light to the probe through a transmitter probe system. The transmitter system includes color separation, beam splitter, and frequency shifter. The output ends of the optical cables are arranged at the fixed positions so the laser beams are parallel to the probe body.

The NIST LDA is a two velocity component system. The laser source is an Argon ion laser operated in multi-color mode. One velocity component uses green light (λ = 514.5 nm) and the second velocity component uses the blue light (λ = 488.0 nm). However, the green light component is used predominately, while the blue light component is used only occasionally for checking the system. Table 1 shows the nominal optical parameters of the LDA probe.

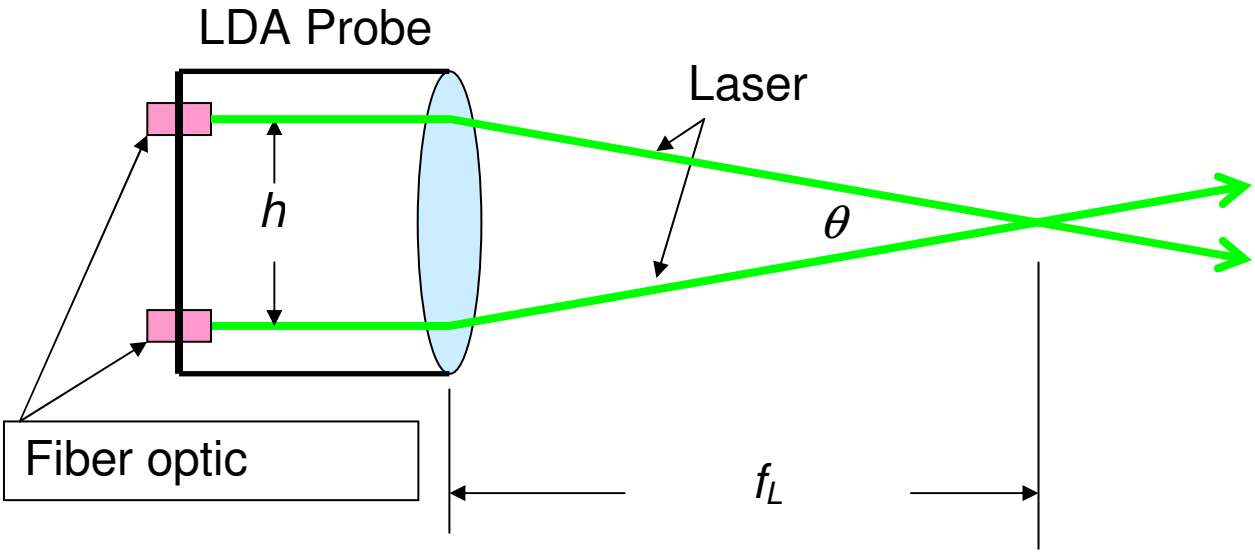

Figure 3 Laser Beams and Their Intersection Angle for 1D Component.

Table 1 Nominal Optical Parameters of the LDA Probe

Laser wavelength λ, nm	514.5
Laser beam separation h, mm	72.5
Focal length f_L, mm	1200
Beam intersection angle θ, deg.	3.46
Fringe spacing d, μm	8.52
Probe diameter d_m, mm	0.3
Probe length l_m, mm	9.9

In the context of airspeed measurement, the average frequency of the scattered light serves as the timer. The particle speed seen by the LDA is

$$V_{LDA} = d\ f_D \tag{3}$$

where f_D is the average Doppler frequency. NIST's LDA system uses a Dantec burst spectrum analyzer (BSA) to determine the Doppler frequency of the scattered light.

At NIST, the light scattering particles used for the airspeed measurements are water droplets injected from the fine air-water sprays located just upstream of the settling chamber of the wind tunnel, as shown in Fig. 1 and Fig. 2.

5.2. Spinning Disk Calibration of Laser Doppler Anemometer

In principle, the speed obtained from Eqn. (3) can be used as primary standard for airspeed measurement if both the fringe spacing d (length scale) and the frequency f_D (timer) are

calibrated at specified uncertainty levels. The value of d can be calculated from the laser wavelength λ and the beam angle θ if both θ and λ are calibrated. However, the calibration of the measured Doppler frequency is still needed to ensure the accuracy of the indicated frequency f_D, which is determined by a Burst Spectrum Analyzer (BSA).

In this work, instead of measuring d and f_D separately, we calibrate the entire LDA system directly by comparing the speed indicated by the LDA to the known speed of a wire attached to a spinning disk unit [5], as shown in Figs. 4 and 5. Similar calibration techniques have been used by others. Dopheide, et al. [6] used the particles on the surface of a thick rotating glass wheel to generate the known tangential velocity. Kurihara, et al. [7] used a rotor with a single wire to simulate the trace particle. Park, et al. [8] used sand paper on a rotating disk to create a known velocity. At NIST, a 5 µm diameter wire is mounted on the rim of a disk of known diameter D. The disk and the light-scattering wire rotate at a measured rotation frequency f_{Disk}, thus enabling the calculation of the tangential speed of the wire from

$$V_{Disk} = f_{Disk}\, D/2 \tag{4}$$

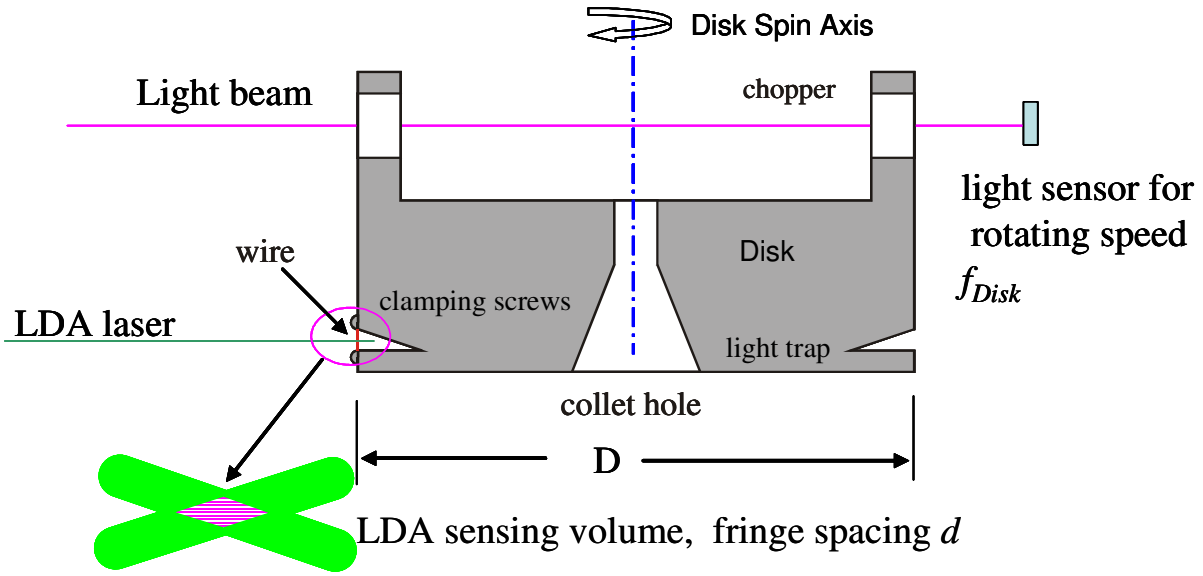

Figure 4 Schematic Diagram of the Spinning Disk for Calibrating the LDA.

The LDA is aligned so that the bisecting plane of the intersecting light beams is parallel to and passes through the axis of the disk and the wire passes through the intersection volume as the disk rotates. In this way, the LDA measures the known speed V_{Disk} produced by the spinning disk. The calibration factor, C_{LDA} is determined from the disk's speed and the speed indicated by the LDA using

$$C_{LDA} = \frac{V_{Disk}}{V_{LDA}} = \frac{D}{2}\,\frac{f_{Disk}}{f_D^C\, d} \tag{5}$$

where f_D^C is the frequency measured by the LDA system when it is scattering from the disk moving at the velocity V_{Disk}. The NIST standard speed thus becomes

$$V_{NIST} = C_{LDA}\, V_{LDA} = \frac{D}{2} f_{Disk} \frac{f_D}{f_D^C} \qquad (6)$$

Thus, the NIST LDA airspeed system is traceable to the length (D) and time standards (f_{Disk}) used in the spinning disk calibration.

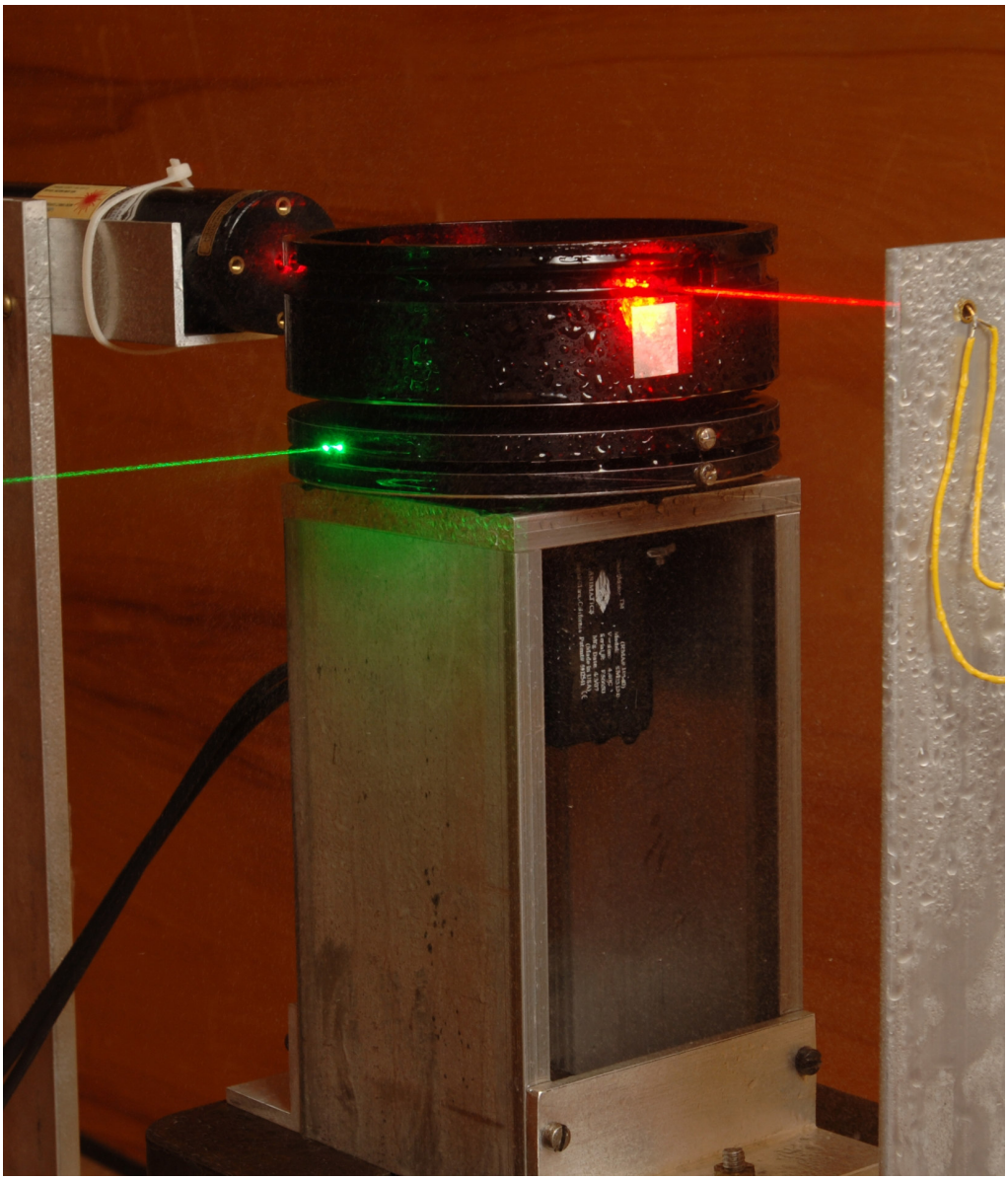

Figure 5 Photo of the Spinning Disk Unit.

5.3 NIST LDA Airspeed Uncertainty Analysis

Here we follow the guidelines for evaluating and expressing uncertainty provided in NIST TN 1297 [9], the ISO Guide [10], and elsewhere [11]. In general, if a measurement quantity, y is a function of variables x_i,

$$y = f(x_1, x_2, ..., x_n) \tag{7}$$

its first-order Taylor series approximation is,

$$dy = \sum_i \frac{\partial y}{\partial x_i} dx_i \tag{8}$$

Thus, the propagation of uncertainty yields

$$\begin{aligned} u_c^2(y) &= \left[\sum_{i=1}^{n} \left(\frac{\partial y}{\partial x_i} \right) u(x_i) \right]^2 \\ &= \sum_{i=1}^{n} \left(\frac{\partial y}{\partial x_i} \right)^2 u^2(x_i) + 2 \sum_{i=1}^{n-1} \left(\frac{\partial y}{\partial x_i} \right) \sum_{j=i+1}^{n} \left(\frac{\partial y}{\partial x_j} \right) r_{ij} u(x_i) u(x_j) \end{aligned} \tag{9}$$

where $u_c(y)$ is the combined standard uncertainty of the measurement result y, $u(x_i)$ is the standard uncertainty of the variable x_i, the partial derivatives $\partial y / \partial x_i$ are the dimensional sensitivity coefficients of x_i on y, and r_{ij} is the cross correlation coefficient between variables x_i and x_j. An alternative form of Egn.(9), which expresses the uncertainty propagation in a dimensionless form, is shown below and it is often more useful.

$$u_y^2 = \sum_{i=1}^{n} c_{x_i,y}^2 u_{x_i}^2 + 2 \sum_{i=1}^{n-1} c_{x_i,y} \sum_{j=i+1}^{n} c_{x_j,y} \, r_{ij} \, u_{x_i} u_{x_j} \tag{10}$$

In Eqn.(10), $u_y = u_c(y) / y$ is the combined dimensionless standard uncertainty of the measurement result y, $c_{x_i,y} = (\partial y / \partial x_i) x_i / y$ are the dimensionless sensitivity coefficients of x_i on y, and $u_{x_i} = u(x_i) / x_i$ is the dimensionless uncertainty of the variable x_i. Equation (10) is used here to estimate the combined uncertainty of the measurement. In many cases, the uncertainty of x_i could not be measured directly. For those cases, the same uncertainty propagation given by Eqn.(10) is used for a sub-measurement process to estimate the combined uncertainty of the sub-measurement. This process is propagated throughout all the measurement components needed until the desired measured quantities are obtained.

According to [9], the sources of uncertainty used in assessing the combined standard uncertainty of the measurement process can be classified according to two types: *Type A* - those which are evaluated by statistical methods, and *Type B* - those which are evaluated by other means. Following this convention, each measured quantity has been classified accordingly as a

u_A or u_B.

Referring to Eqns.(6) and (10), the airspeed uncertainty depends on the uncertainties of the variables of the diameter of the rotating cylinder D, the rotating frequency f_{Disk}, and the Doppler frequencies measured by the LDA system f_D^C and f_D. Although not shown in Eqn. (6) explicitly, many other variables could affect the uncertainties of the airspeed measurements. Based on the theory for the uncertainty propagation given above, the uncertainty from the sub-variable components is estimated and included in the uncertainty of the NIST airspeed measurement. In addition, the result given in Eqn. (6) is based on the assumption of a perfect alignment. The misalignment of the LDA and disk will produced additional uncertainty. These sub-variables and additional uncertainties are discussed in detail in following sections. The sources and values of the uncertainties of these variables are summarized in Table 2, as well as their classification as either u_A or u_B. The corresponding airspeed uncertainties due to these sources are also given in Table 2.

5.3.1 The diameter of rotating cylinder, *D*

In the NIST facility, the light-scattering wire is a tungsten wire 5 μm in diameter. The wire is mounted by clamping screws to the curved surface of the short right circular cylinder shown in Fig. 4 and 5. The wire is parallel to the axis of the cylinder. The wire spans a groove machined into the cylinder, shaped to serve as a light trap to eliminate unwanted reflected laser light. A hole along the axis of the cylinder is shaped to receive a small collet to facilitate mounting the cylinder on the shaft of gear motors. Care was exercised in the machining process to assure that the collet hole and the curved surface of the cylinder are coaxial. The cylinder is mounted on the output shaft of a gear motor such that the cylinder rotates in a horizontal plane. The entire assembly is mounted on an *x-y* translation stage. The diameter of the cylinder was measured to be 136.522 mm with a standard uncertainty of 0.005 mm or 0.0037 % using a triple axis coordinate measuring machine (see uncertainties in Table 2). This will give 0.0037 % uncertainty in speed measurements.

5.3.2 The thermal expansion of the disk

The diameter of the disk D changes with the temperature. The temperature at which the diameter was measured might be different from the temperature where the diameter is used for LDA calibration. When the linear thermal expansion of the disk is assumed to be 1.7×10^{-5} /K, the change in D is 0.0116 mm or 0.0085 % for a 5 K difference in the temperature change. This contributes 0.0085 % uncertainty in speed.

5.3.3 The thermal expansion of the probe

Although fringe spacing d is not explicitly shown in Eqn. (6), its uncertainty will affect the uncertainty of the burst frequency measurement. The dimension of the probe and the beam separation h and the fringe spacing d will change with the temperature. The housing of the probe

is made from aluminum and its linear thermal expansion is assumed to be 1.7×10^{-5} /K. Referring to Eqns. (1) and (2), and the optical parameters of the probe given in Table 1, for a 5 K difference in temperature, the change in h is 0.0062 mm and in d is 0.00071 μm or 0.0085 %. Here, we have assumed that the temperature change does not affect the alignment of the two laser beams and that the beams are kept parallel to the probe body all the time. Since the uncertainty of d affects both the uncertainties of f_D^C and f_D, the total uncertainty on speed due to d is $\sqrt{2} \times 0.0085$ % = 0.012 %. Here the Type A variations of f_D^C and f_D are assumed to be independent.

5.3.4 The frequency counter of the rotating disk

Calculation of the wire speed requires the measurement of the rotation frequency of the disk. This frequency is measured by counting the pulses produced by an optical signal modulated by the rotating disk. As shown in Fig. 4 or 5, the top surface of the disk was hollowed out so that the disk resembles a straight-sided bowl with a thick bottom. The side wall of the bowl has two holes, one centered on each end of a diameter through the axis. These holes serve as an optical chopper for a helium-neon laser, positioned so its light beam strikes a photo diode when the holes are aligned with the laser and the photo diode. This setup produces two pulses for each rotation. The output of the photo diode is counted with a frequency counter that determines the rotation rate of the disk. The frequency counter has a Type A uncertainty of 0.31 parts in 10^6 and a Type B uncertainty of 1.55 parts in 10^6. For a clock frequency of 1 MHz, this will give a Type A uncertainty of 3.2×10^{-5} % for a typical measurement time of 60 s and Type B uncertainty of 0.0002 %.

5.3.5 The motor speed variation

A single Animatics Smart Motor, Model SM2315D with Animatics power supply Model PS42V6AG-110 was used to drive the calibration disk. The motor is digitally integrated motion controlled. It provides stable rotation rates in very large rotating range and has an encoder with a resolution of 2000 counts per revolution. The standard deviation of the disk rotation speed is found to be 0.038 % in the operation range.

5.3.6 Variation of fringe spacing with position

When the Gaussian laser beam is focused by a lens, the minimum beam diameter (the waist) is found at the back focal plane of the lens only if a waist also exists at the front focal plane. Interference fringes are formed in the volume where both laser beams intersect. If both beam waists are not located at this intersection, an enlarged probe volume at some part in the volume will result [3, 4]. Since the waists do not occur exactly at the intersection usually, the spacing of the interference fringes is not constant throughout the sensing volume as shown in Fig. 6. This error can be significant when the frequencies of the observed 'Doppler' signals are related to the speed of the scattering particles passing through the different parts of fringes. When fringe spacing is not constant throughout the probe volume, a constant wire speed will produce different LDA Doppler frequencies when the wire is located at different locations (see the value x_w in Fig. 9). Fig. 7 shows an example of the variation of the measured indicated velocity as a function of

the wire location. The data show that the measured velocity is a linear function with the wire location within the sensing volume (-3 mm to +3 mm on the graph). Therefore, particles passing through different locations will produce different speeds indicated by the LDA, even when their speeds are the same just as the rotating disk does (Fig. 4). In the NIST standard, the averaged speed indicated for all particles passing the sensing volume is assumed to be the system speed for the LDA calibration. This assumption is reasonable because: (1) the variation of the speed ratio is linear, and (2) the particle concentration is uniform throughout the sensing volume so the probability of the LDA signals produced by particles is symmetric about the center point.

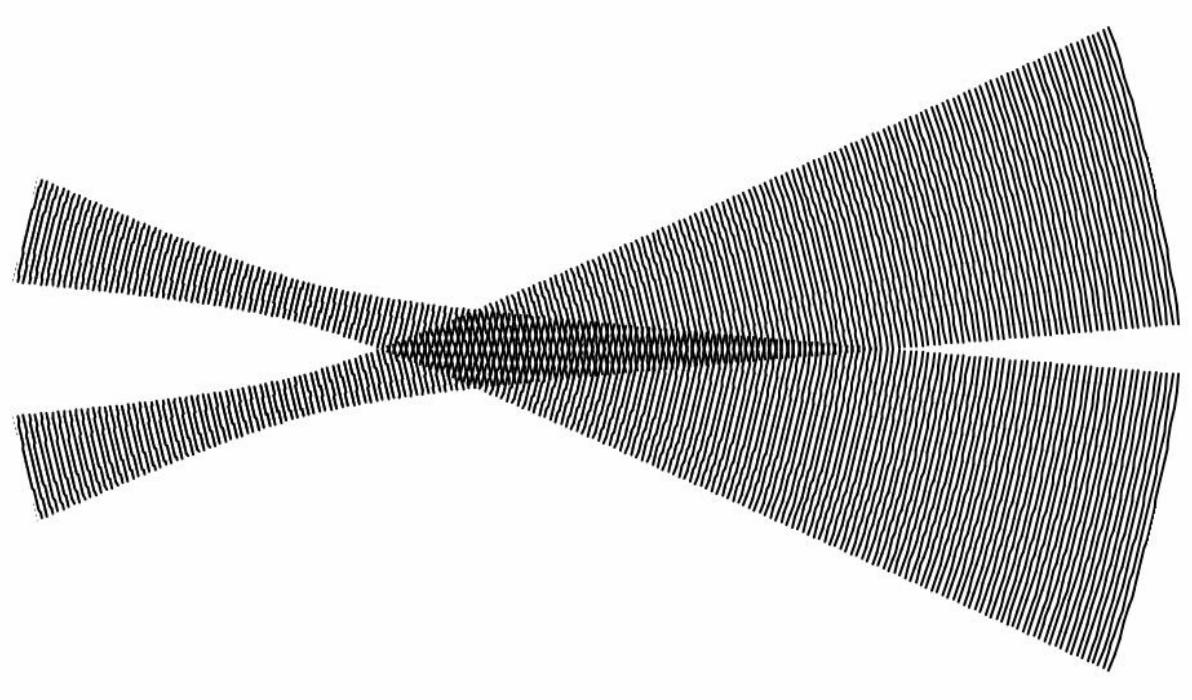

Figure 6 Fringe Spacing Variations in an Improperly Aligned System

To determine the mean value of the calibration, a least square error linear curve was obtained for each tested speed. The straight line shows the fitting of the data. From the fitted curve, both the mean value and the standard deviation of the LDA-disk calibration are obtained. The standard deviation obtained from the fitting will be discussed in the next section. The mean value is the speed calibration factor, C_{LDA} as described in Eqn. (5). The variation of the mean values at different time and different speeds are mainly due to the uncertainty of locating the wire position with respect to the probe volume. The variation of the mean value is particularly true when the fringe spacing is not constant throughout the probe volume as discussed above. The standard deviation of this mean value is found to be 0.13 %. This is classified as the uncertainty from the fringe space variation.

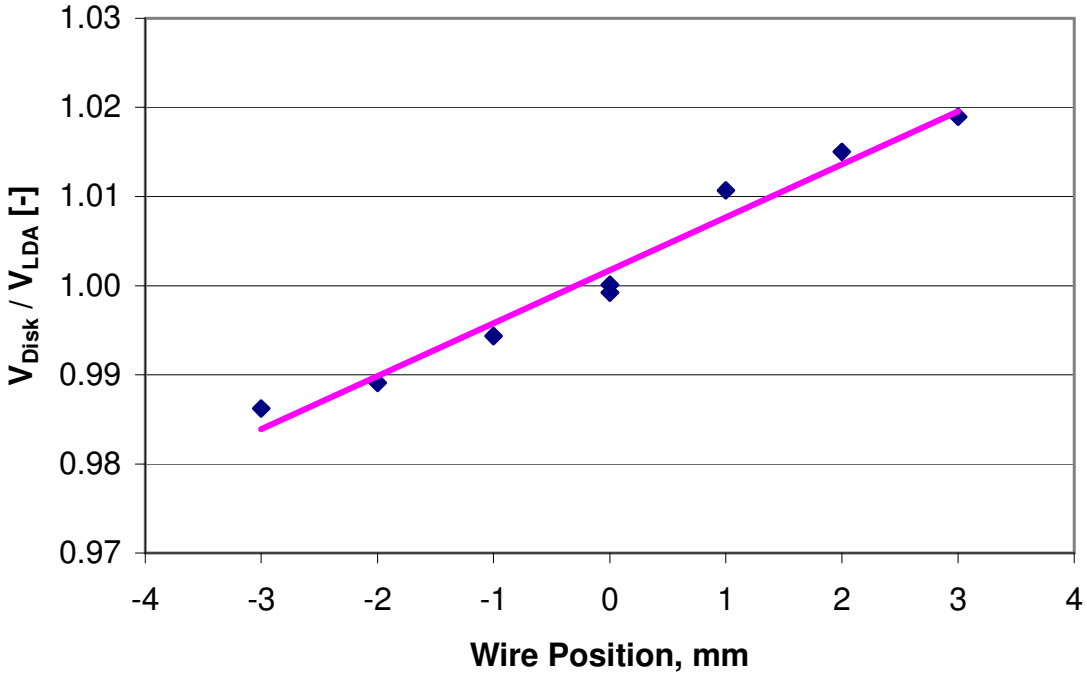

Figure 7 LDV Calibration Results vs Wire Position.

5.3.7 The burst spectrum analyzer

Frequency, f_D^C or f_D, is determined by a burst spectrum analyzer (BSA). The uncertainty of the BSA consists of the uncertainty resulting from the clock (oscillator) used for time scale and the uncertainty from the BSA designed to interpret the burst frequency. The sensitivity coefficients of f_D^C and f_D for airspeed are -1 and +1, respectively. So that the systematic uncertainty of the BSA will be cancelled out on the airspeed uncertainty while the Type A uncertainty on the airspeed will be enlarged by a factor of $\sqrt{2}$.

The clock used for the frequency or time scale has a Type A uncertainty of 0.5 parts in 10^6 and a Type B uncertainty of 2 parts in 10^6. For the nominal fringe space of 8.52 μm, the Type A and B uncertainties are $5\text{x}10^{-5}$ % and 0.0002 %, respectively. Thus the resulting uncertainty on speed due to the clock is $\sqrt{2}$ x $5\text{x}10^{-5}$ % =$7.1\text{x}10^{-5}$ % for the Type A uncertainty and is zero for the Type B uncertainty due to cancellation.

The estimation of the other uncertainties for the BSA is more complicated. We have estimated these uncertainties from the uncertainty of the disk-LDA calibration. This uncertainty is identified by the standard deviation obtained from the curve fitting as discussed in section

5.3.6 and shown in Fig. 7. The uncertainty as a function of the calibrated speed is plotted in Fig. 8. Diamond symbols shown in Fig. 8 are the combined uncertainty of the disk-LDA calibration data. This uncertainty is mainly due to both the disk rotation speed and BSA uncertainties. Since the systematic uncertainty is cancelled out for the final speed measurement and is not the issue here, the data shown is only for the Type A uncertainty. The disk-LDA uncertainty data can be represented by two independent terms: a constant speed term and a constant ratio term. These two terms were found by fitting curve to the data in Fig. 8 and the result of the fitting, $((0.13/V)^2 + (0.21)^2)^{1/2}$, in %, is shown as the solid curve. The constant speed term (the speed uncertainty for any speed) is 0.0013 m/s (corresponding to a 150 Hz on the BSA for an 8.52 μm fringe spacing) and the constant ratio term is 0.21 % of the speed. The constant speed term (0.0013 m/s) results from the resolution of the BSA while the constant ratio term results from the combined effect of the motor speed variation and the conversion factor of the BSA.

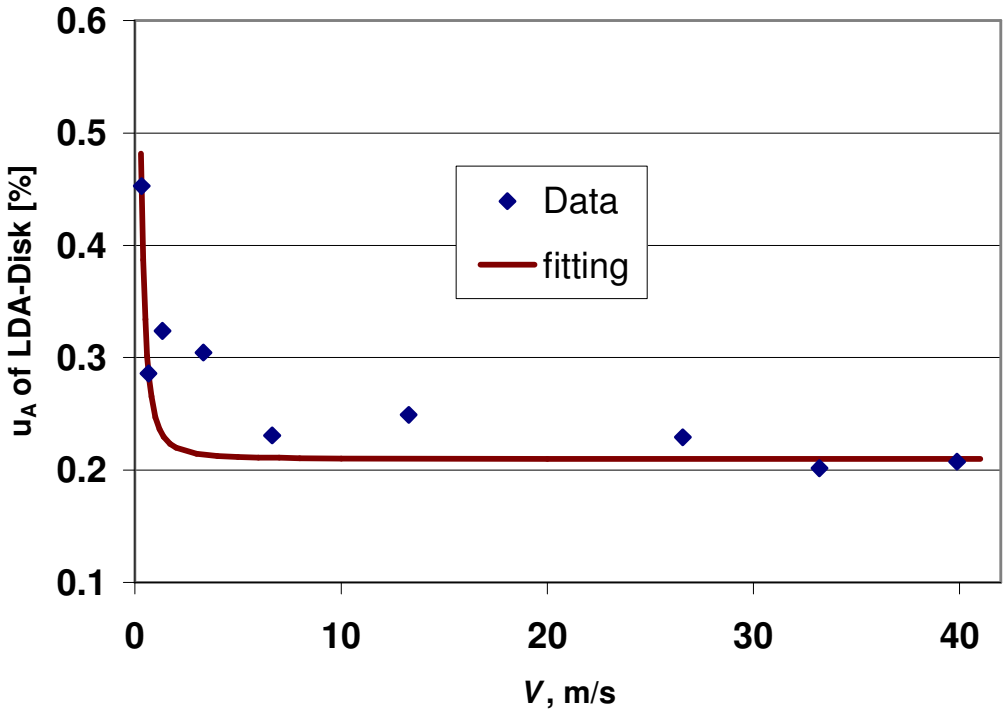

Figure 8 Type A Uncertainty of LDA-Disk Calibration. The fitting is $((0.13/V)^2 + (0.21)^2)^{1/2}$ in %.

The BSA uncertainty can be estimated by subtracting the motor speed uncertainty of 0.038 %, found in Section 3.5, from the combined uncertainty (accounting for the RSS relationship). Here we have assumed that the motor speed uncertainty is independent of the BSA uncertainty. The resulting BSA uncertainty for the constant percentage term is thus 0.207 % ($= (0.21^2 - 0.038^2)^{1/2}$ %). It is the uncertainty of the conversion factor of the BSA.

The Type A uncertainty of the BSA affects both f_D^C and f_D independently and thus the resulting speed uncertainty is $\sqrt{2}$ x 0.0013 m/s = 0.0018 m/s for the constant speed term and $\sqrt{2}$ x 0.207 % = 0.29 % for the constant percentage term.

5.3.8 Angle Misalignment for LDA-Disk calibration

As noted above, the result given in Eqn. (6) is based on the assumption of a perfect alignment. The misalignment of the LDA and disk will produce additional uncertainty. The rotating disk is mounted on the output shaft of a gear motor such that the disk rotates with a vertical spin axis. The entire assembly is mounted on an x-y translation stage. The alignment of LDA probe with the direction of the wire velocity is another parameter to be examined. As noted above, the LDA must be aligned so that the plane bisecting the intersection angle is parallel to and passes through the axis of the cylinder. Fig. 9 shows the local coordinates for the disk and the laser beams intersection during the LDA-Disk calibration. The laser beams are on an x-y plane and z is normal to the x-y plane. The center of the probe volume is assumed to be at the coordinate origin, (0,0,0). The light scattering wire is located at x_W, oriented in the z direction and moves in the y direction when the disk is rotating. $\boldsymbol{n}$ is a unit vector normal to the bisecting plane (x-z plane). The fringes are parallel to the bisecting plane. ϕ is the angle between the wire velocity V_{DISK} and the unit vector, $\boldsymbol{n}$. C is the axis of the rotating disk.

To help making the alignment of the LDA with the disk, an acrylic rod having a 1 mm diameter hole drilled along the axis of the rod is mounted vertically in the hole on top of the collet of the disk. The LDA is aligned with the axis by *x-y* translations of the cylinder assembly so that the intersection volume is centered on the axis of the acrylic rod (*C* in Fig. 9). The 1 mm hole scatters light and makes the laser light visible on the axis. The x-y translations are adjusted for maximum brightness of the scattered light. The traversing system on which the fiber optic probe is mounted is then backed away a distance equal to the radius of the cylinder and lowered so that the wire passes through the intersection volume as the cylinder rotates. To ensure the bisecting plane of the laser beams is always in line with the disk axis when the traversing system is moved, the bisector of the laser beams (the optical probe) must be aligned with the traversing system correctly. The alignment can be checked by turning the probe 90^o to have a vertical bisecting plane and then checking the intersection while moving the traversing system. Final adjustment is done by turning the lead screw of the traverser slowly while watching the input to the signal processor on an oscilloscope. When the system is misaligned, the observed speed is given by $V_{Disk}\ \cos(\phi)$. The uncertainty of the calibration speed is the cosine effect of the misalignment. It is 1-cos(ϕ) for an angle of ϕ. The misalignment angle ϕ can be decomposed into two orthogonal angles, ϕ_x and ϕ_z. The uncertainties of the misaligned angles are estimated to be 0.5 deg. and thus a speed uncertainty of 0.004 % for both ϕ_x and ϕ_z.

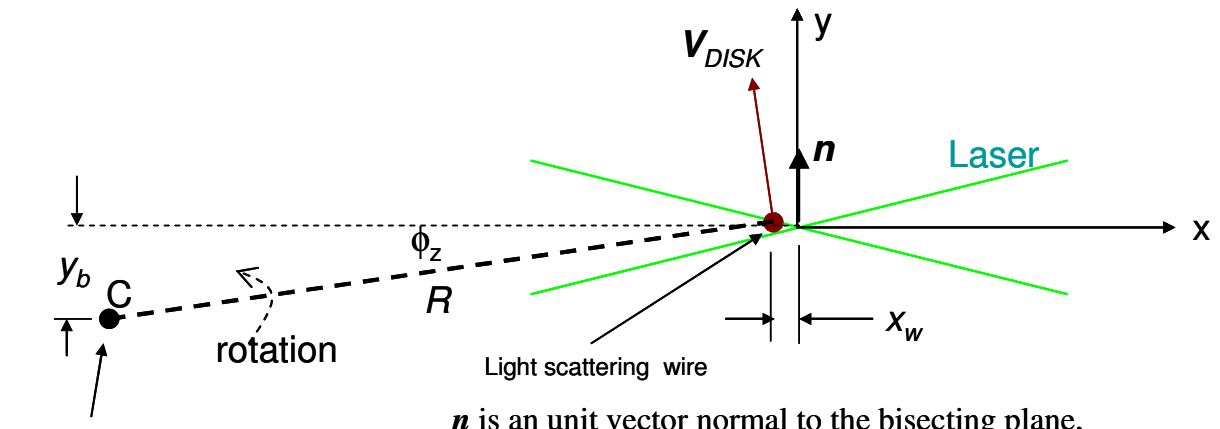

Axis of the rotating disk. *R* is the distance between the wire and the axis

n is an unit vector normal to the bisecting plane, ϕ is the angle between $\boldsymbol{V}_{\mathrm{DISK}}$ and ***n***. ϕ_x (not shown) and ϕ_z, are the components of the angle ϕ rotated around *x* and *z* axes respectively.

Figure 9 Local Coordinates for the Spinning Disk and the Laser Beam Intersection.

5.3.9 Misalignment in LDA with wind tunnel installation

The sources of the uncertainties discussed above are only for the LDA airspeed standards system. However, additional uncertainties must be added if the LDA probe is not aligned with respect to the airspeed direction in the test section of the wind tunnel or if the device under test is misaligned. Ideally, the unit vector of the bisecting plane should be in the direction of the airspeed (y). That is, the laser bisecting plane should be in vertical direction (z) and parallel to the *x* direction (horizontal and normal to y). α_x and α_z denote the angles of misalignment rotated around the *x* and z axes, respectively. The airspeed uncertainty due to the cosine effect varies with 1-cos(α_x) and 1-cos(α_z). The uncertainties of these misaligned angles are estimated to be 1 deg. and thus a speed uncertainty of 0.015 % for both α_x and α_z.

5.3.10 Summary of the NIST airspeed standards uncertainty

Table 2 lists the sources and values of the uncertainties. Table 3 lists the effect of the source uncertainties on the uncertainty of the NIST airspeed standards. As shown in Table 3, the major uncertainty of the airspeed standards is due to the BSA uncertainty given in section 5.3.7 and the variation of fringe spacing given in section 5.3.6.

The airspeed uncertainty is classified into two types: a constant speed term and a constant percentage term as shown in Table 2. The uncertainty for each group is then combined and given in Table 3.

Table 2 Summary of Sources and NIST Airspeed Uncertainties.

Variable Sources	Section	Sources			Speed Uncertainty	
		Mean	u_a	u_B	u_A %	u_B %
Diameter of rotating disk, D [mm]	5.3.1	136.5	0	0.005	0	0.0037
Thermal expansion of D, [mm]	5.3.2	136.5	0.0116	0	0.0085	0
Fringe spacing expansion, d [μm]	5.3.3	8.52	0.0007	0	0.012	0
Timer for rotating disk [parts in 10^6]	5.3.4	-	0.31	1.55	$3.2\text{x}10^{-5}$	0.0002
Rotation speed, [%]	5.3.5	-	0.038	0	0.038	0
Fringe spacing with position, [%]	5.3.6	-	0	0.13	0	0.13
Clock for BSA [parts in 10^6]	5.3.7	-	0.5	2.0	$7.1\text{x}10^{-5}$	0
BSA constant speed term [m/s]	5.3.7	-	0.0013	0	$0.18/V_{LDA}$	0
BSA constant ratio term [%]	5.3.7	-	0.207	0	0.29	0
LDA-disk, ϕ_x , [deg]	5.3.8	0	0	0.5	0	0.004
LDA-disk, ϕ_z , [deg]	5.3.8	0	0	0.5	0	0.004
LDA-wind tunnel, α_x, [deg]	5.3.9	0	0	1.0	0	0.015
LDA-wind tunnel, α_y , [deg]	5.3.9	0	0	1.0	0	0.015

Table 3 Combined Airspeed Uncertainty

	u_A %	u_B %
Constant ratio term	0.29	0.13
Constant speed term	$0.18/V_{LDA}$	0

Based the data in Table 3, the results for the total combined standard uncertainty for the NIST airspeed, in m/s can be given as

$$u_c(V_{NIST}) = \sqrt{(0.0029 V_{LDA})^2 + (0.0013 V_{LDA})^2 + (0.0018)^2} \qquad (11)$$

where V_{LDA} is in m/s. The approximate confidence level of the result given above is 68 %. Following the guidelines of [9], the expanded uncertainty with a coverage factor k is given as

$$U(V_{NIST}) = k\sqrt{(0.0032\,V_{LDA})^2 + (0.0018)^2} \tag{12}$$

When a coverage factor of $k = 2$ is used to convert the combined standard uncertainty to an expanded uncertainty, with an approximate 95 % level of confidence, the expanded uncertainty, in m/s, becomes:

$$U(V_{NIST}) = \sqrt{(0.0064\,V_{LDA})^2 + (0.0036)^2} \tag{13}$$

Based on Eqn. (13), the NIST airspeed expanded uncertainty is plotted in Fig. 10 in the unit of m/s for the coveraged airspeed range of 0.15 m/s to 40 m/s. This gives a minimum uncertainty of 0.0038 m/s at the lowest airspeed of 0.15 m/s and a maximum uncertainty of 0.26 m/s at the highest speed of 40 m/s. The uncertainty from the spinning disk can be obtained by removing the BSA uncertainty given in section 5.3.7 and alignment uncertainty given in section 5.3.9 and is shown as dashed line in Fig. 10 for reference. The same uncertainty data are plotted in Fig. 11 in the unit of %. This gives a maximum uncertainty of 2.5 % at the lowest airspeed of 0.15 m/s and a minimum uncertainty of 0.65 % at the highest speed of 40 m/s.

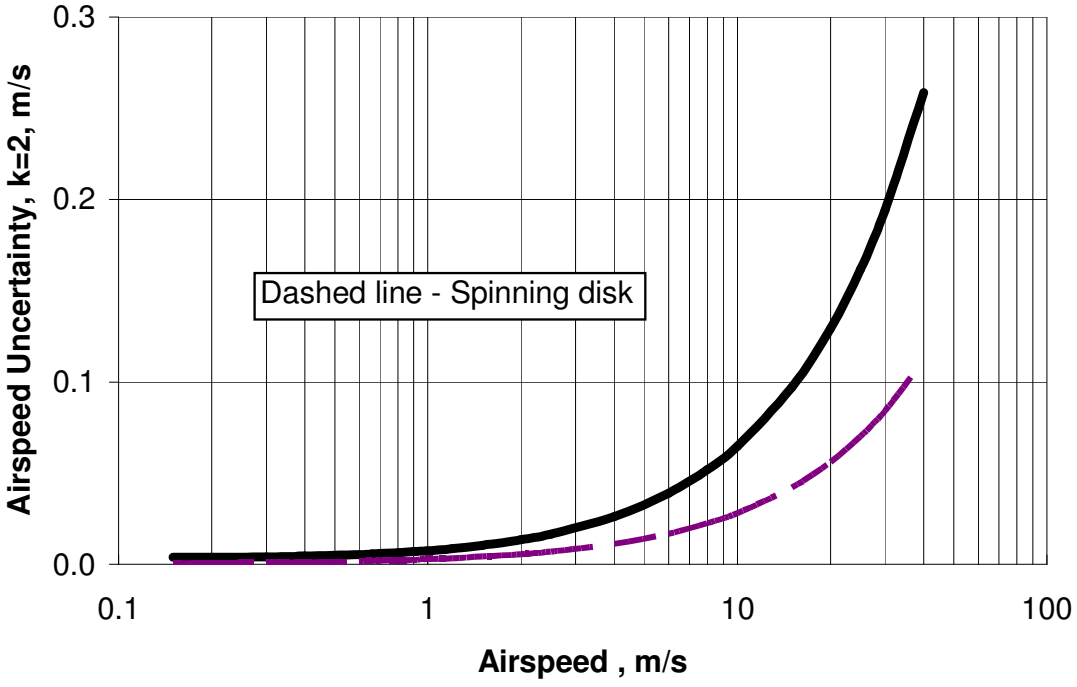

Figure 10 NIST Airspeed Uncertainty in m/s versus Airspeed

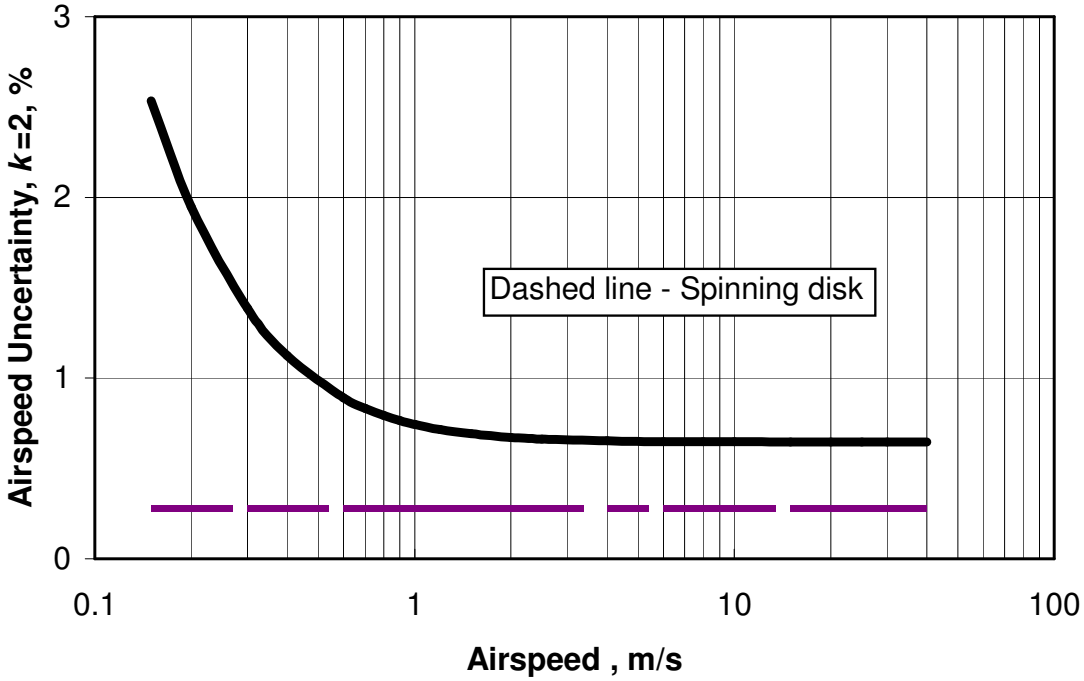

Figure 11 NIST Airspeed Uncertainty in % versus Airspeed

5.4 Uncertainty of Airspeed Calibration

The uncertainty analysis reported here is for the NIST airspeed standards. To obtain the uncertainty for an airspeed meter calibration additional uncertainties, such as the alignment uncertainty of the meter should also be included. The LDA measures the airspeed directly in varying environmental conditions (temperature, pressure, and humidity). Some airspeed sensors might be greatly affected by the environmental conditions and they require corrections of the environmental effects on the indicated speed. The uncertainty for the IUT results will also depend on the airspeed sensor type, and the associated instruments used during the airspeed calibration. In addition, the quality of the water drop seeding used for LDA could also affect the LDA data rates and uncertainty. To account for these additional uncertainties, the expanded uncertainty of the calibration of the instrument under test, U , can be calculated by

$$U = k\sqrt{u_{V_{NIST}}^2 + u_{Acq}^2 + u_R^2} \qquad (14)$$

The quantity $u_{V_{NIST}}$, as given in Eqn. (14), is the standard uncertainty of the airspeed measurements made with the LDA as discussion in section 5 above. The quantity u_{Acq} is the standard uncertainty of the data acquisition system and instrumentation used to obtain the readings from the instrument under test. In this case, the uncertainty due to data acquisition is considered negligible. The quantity u_R is the reproducibility [12] of the test. Reproducibility is herein defined as the closeness of agreement between measurements with the airspeed changed

and then returned to the same nominal value. To measure the reproducibility of the test, u_R, the standard deviation of the air speed ratio at each of the nominal air speeds was used to calculate the relative standard uncertainty. By using this method, the total uncertainty of the calibration data for the test meter will include both contributions from the calibration system and IUT.

6. Check Standards

Beside the LDA used as the primary airspeed standard, NIST maintains the airspeed check standards: the Pitot-static tube probe (pst) and thermal anemometer (Ta). Current check standard results are compared to prior results as a means of verifying the continued proper operation and performance of all of the air speed calibration service systems (instrument calibrations, software, operating procedures, the check standards themselves, etc.). The check standards are also used if there is any significant change made to the system or before a critical calibration.

6.1. Pitot-Static Tube

Henri de Pitot first described the instrument that bears his name in 1732 [13, 14]. Currently, the Pitot-static tube, or Pitot tube, is still widely used to measure the speed of gas and liquid streams. The operation principle of a pst is based on the well known Bernoulli's equation. For an incompressible flow, the Bernoulli's equation [15] gives

$$P_t = P_s + \frac{1}{2}\rho V^2 \tag{15}$$

where P_t is the total pressure, P_s is the static pressure, and $\frac{1}{2}\rho V^2$ is the dynamic pressure for a fluid of density of ρ and flow speed of V. Solving for the velocity, we have

$$V = C_D \sqrt{\frac{2\,\Delta P}{\rho}} \tag{16}$$

where C_D is added to denote the pitot-static meter constant, and $\Delta P = P_t - P_s$ is the differential pressure between the total pressure and the static pressure, or the dynamic pressure.

The density of the air, in kg/m^3, is calculated with the expression [16]

$$\rho = \frac{c0}{T}\left(P - c1\,H\,c2\,e^{\frac{-C3}{T}}\right) \tag{17}$$

where the constants c0 = 0.003 484 8, c1 = 0.003 796, c2 = 1.7526x10^{11}, and c3 = 5315.56, T is the absolute air temperature in °K, P is the barometer pressure in Pa, and H is the relative humidity expressed as a percent.

Fig. 12 is a sketch of a typical version of the device. It is comprised of two concentric tubes. The center tube is open; the annular space between the tubes is sealed at one end. There is a band of small, radial holes through the wall of the outer tube located about eight outer tube diameters from the sealed end. The tubes are oriented parallel to the direction of the flow with the sealed end facing into the flow. The other ends of the tubes are connected to instrumentation to measure the differential pressure between that in the center tube and that in the annular space. The center tube senses the total pressure that is the sum of the static ambient pressure and the pressure due to the motion of the fluid. The radial holes sense only the static, ambient pressure. The differential pressure is due to the motion of the fluid. Often, the multi-port averaging Pitot-static tube is an appropriate choice as the primary element for measuring the differential pressure.

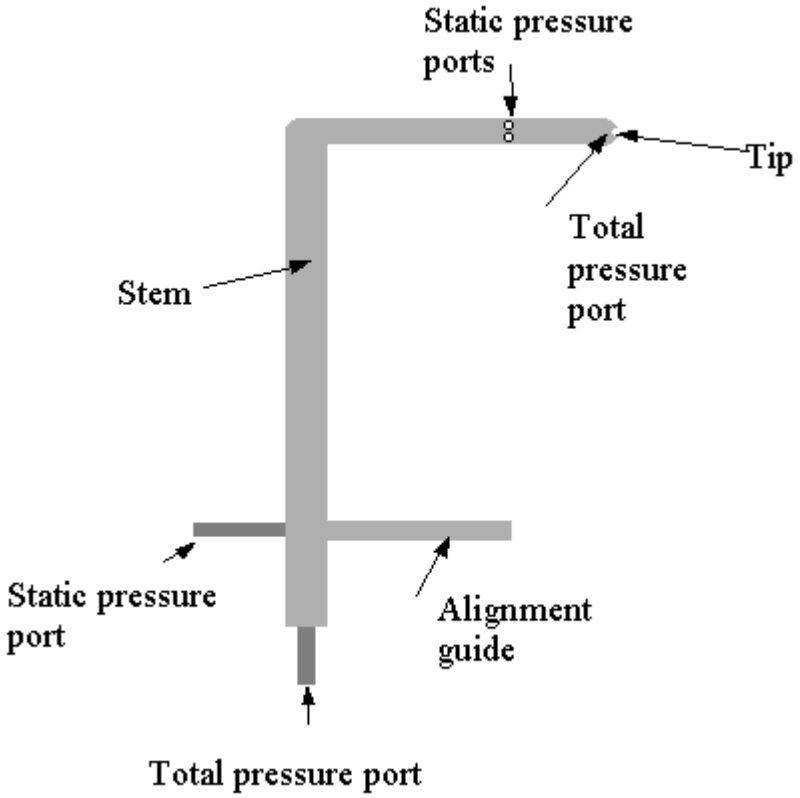

Figure 12 Sketch of a Pitot tube.

A Pitot-Static tube provides the measurement of dynamic pressure allowing calculation of the flow velocity. However, a Pitot-static tube alone can not provide the air speed information. The airspeed is only calculated from the measured dynamic pressure (ΔP) and the air density. The pst velocity error is mainly due to inaccurate sensing of static pressure. It is usually not possible to find locations for the static ports which accurately sense static pressure at all speeds and angles of attack. The pst is a square root device, meaning the square root of the ΔP is proportional to the flow speed. Thus it produces a very small ΔP and a large speed uncertainty at low velocity (< 1 m/s for air).

The NIST pst system is calibrated periodically with the LDA system. The sample calibration data for the air speed ratio, $Y = V_{NIST} / V_{pst}$, taken in a period of a year, are shown in Fig. 13. Without calibration, the typical standard uncertainty of Pitot-static probes is about 1.5 %. Based on the calibration, a curve fitting of $Y = 0.992\ 011 + 5.001 \times 10^{-5}\ V_{pst}$ is obtained and shown as solid line in the Fig. 13. The deviation of the speed ratio from the fitting is shown in Fig. 14. The typical standard uncertainty of the calibrated pst probe is about 0.35 %.

Traditionally, uncalibrated psts were often used as airspeed standards. The calibrated pst can also be used as an airspeed transfer standard. Currently, NIST uses the pst as a check standard.

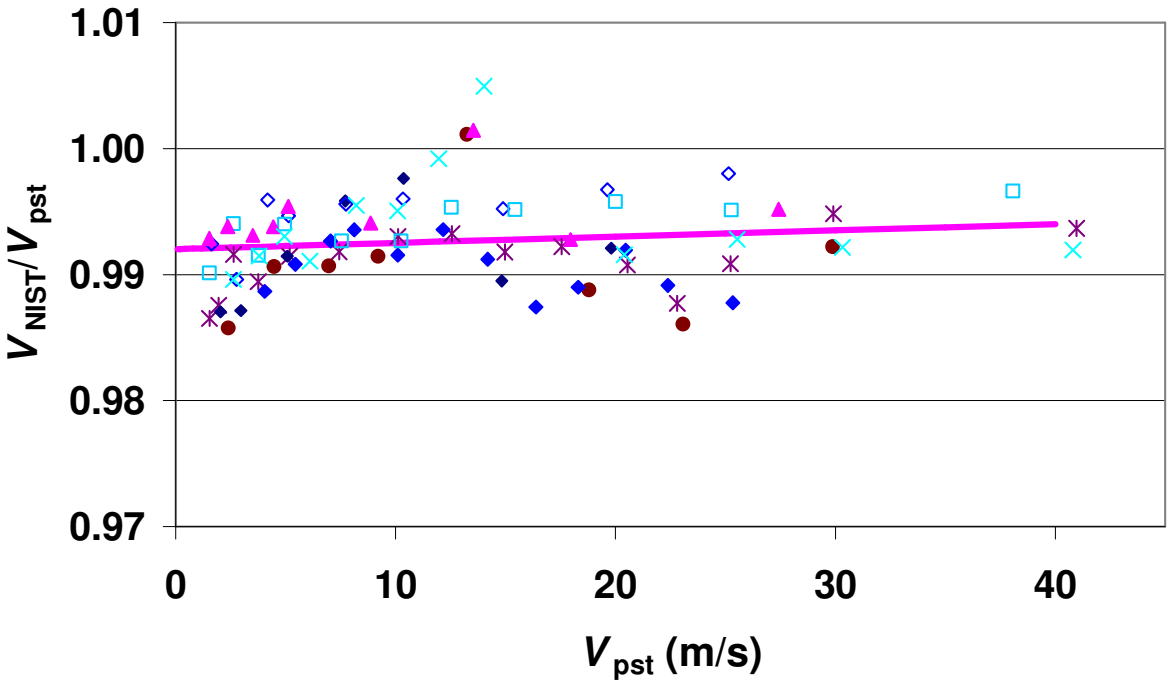

Figure 13 NIST Pitot Static airspeed vs. NIST Standard airspeed. Data taken between 4/12/05 and 2/1/06. Solid line is a curve fit.

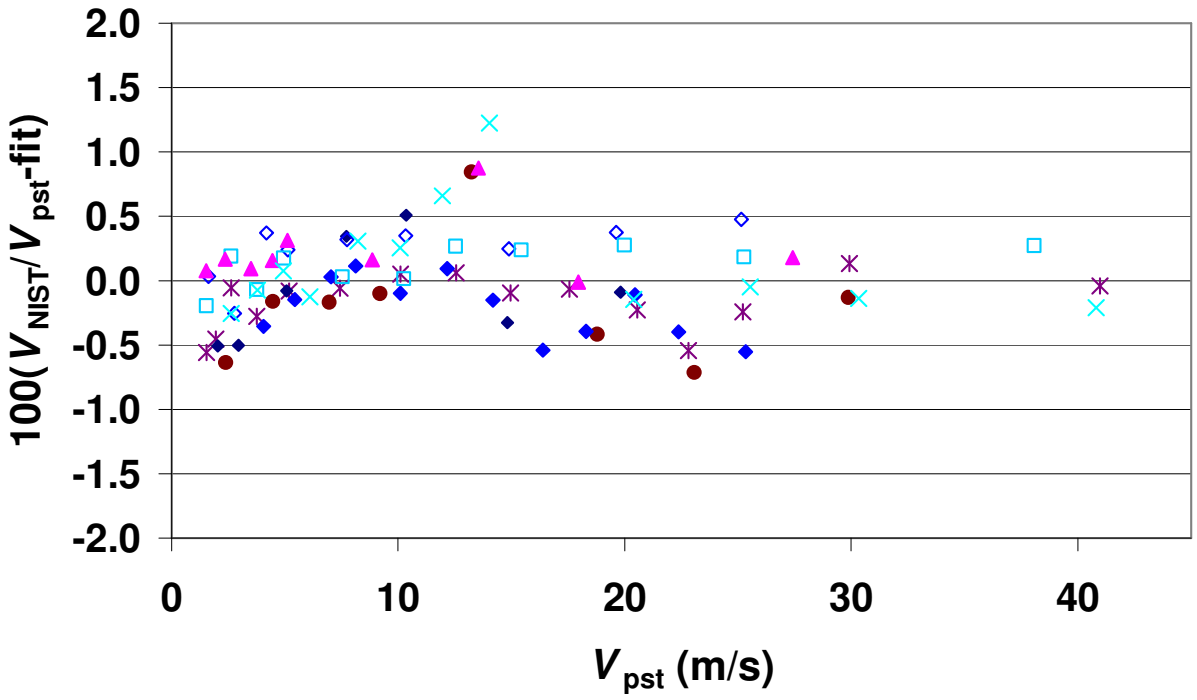

Figure 14 Deviation of the speed ratio Y for the pst probe from the curve fit. Data taken between 4/12/05 and 2/1/06.

6.2. Thermal Anemometer

A thermal anemometer (Ta) is an instrument for determining fluid velocities by measuring heat transfer from a small, electrically-heated wire or film sensor immersed in the fluid [14, 17]. The rate at which heat is removed from the sensor is related to the velocity of the fluid flowing over the sensor. Therefore, the fluid velocity is related to the current or voltage required to maintain the sensor at a constant temperature. Since the heat transfer rate depends on many details of the construction of the sensor, it is difficult to get an analytical expression for this relationship. Therefore, NIST periodically calibrates the Ta that is used as a check standard for the airspeed measurements. These calibrations use the LDA system. The calibration data for the air speed ratio, $Y = V_{LDA} / V_{Ta}$ are shown in Fig. 15. At constant airspeed, the typical standard deviation is approximately 1 %. But the nonlinearity with the speed could contribute a larger airspeed uncertainty of about 4 %, especially at low speeds. From the calibration data, a curve fitting based on the format $y = (a + c\,x + e\,x^2 + g\,x^3)/(1 + b\,x + d\,x^2 + h\,x^3)$, where $x = \log(V_{Ta})$ is obtained and shown as a solid line in the Fig. 15. The deviation of the speed ratio from the fitting is shown in Fig. 16. The typical standard uncertainty of the calibrated Ta probe is about 1.2 %.

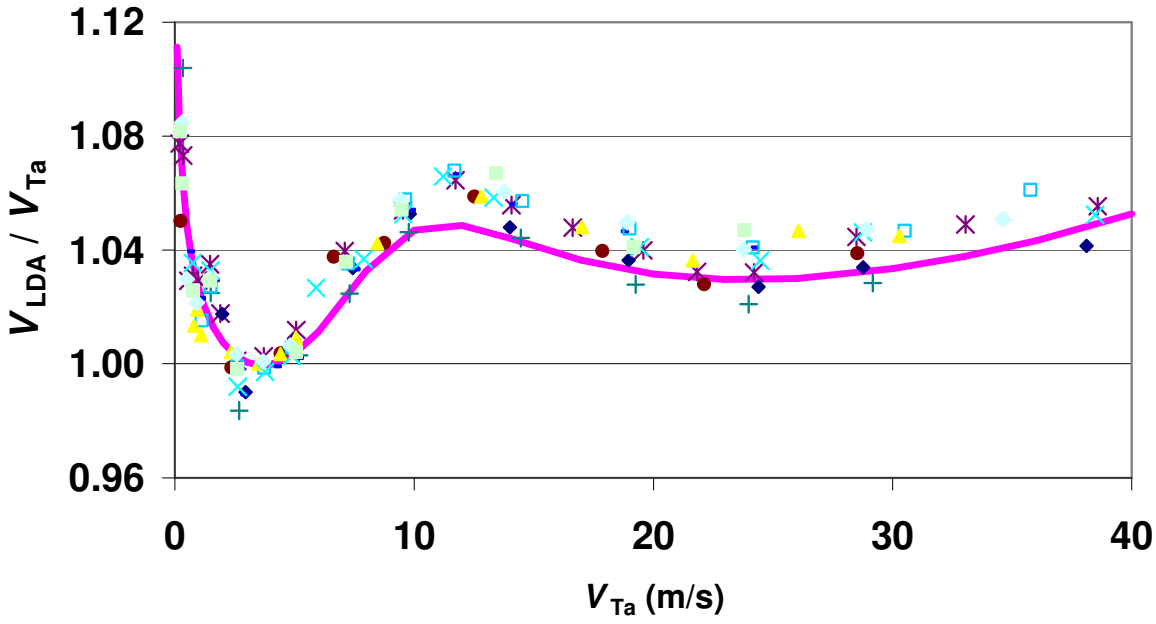

Figure 15 NIST Ta airspeed vs. NIST Standard airspeed. Data taken between 4/12/05 and 4/5/06. Solid line is a curve fit.

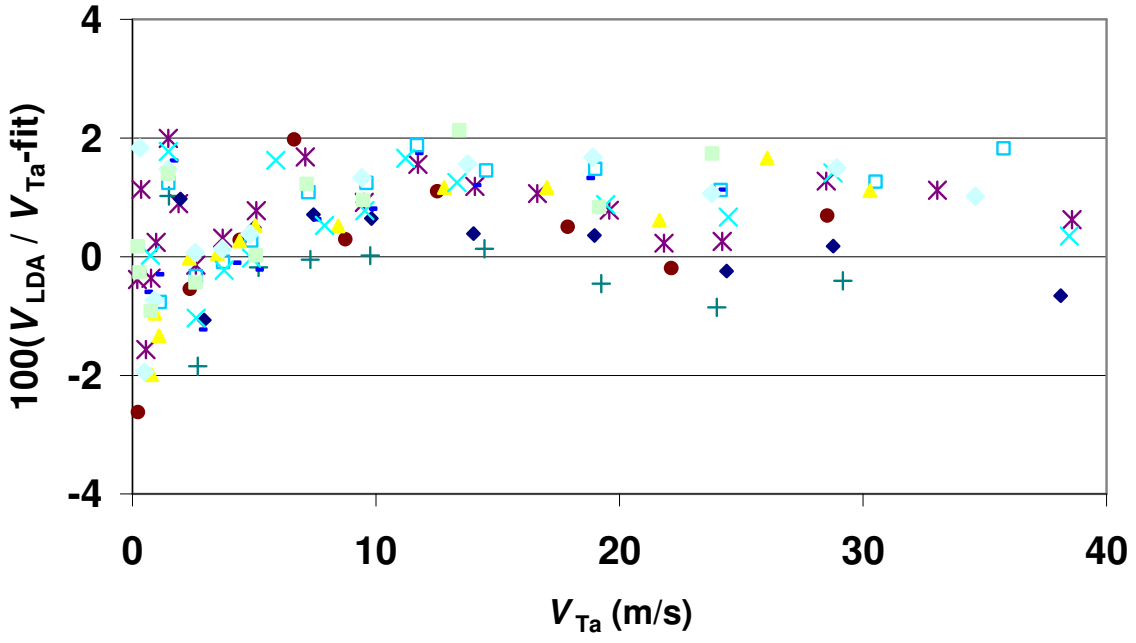

Figure 16 Deviation of the speed ratio Y for the Ta probe from the curve fit. Data taken between 4/12/05 and 4/5/06.

References

[1] NIST Calibration Service Users Guide 1998, J.L. Marshall, Editor, NIST Special Publication 250, January 1998, National Institute of Standards and Technology, Gaithersburg, MD.

[2] Mease, N.E., Cleveland, W.G., Mattingly, G.E. and Hall, J.M., "Airspeed Calibrations at the National Institute of Standards and Technology", Proceedings of the Measurement Science Conference, Anaheim, CA 1992.

[3] Durst, F., Melling, A. and Whitelaw, J.H. "Principles and Practice of Laser-Doppler Anemometry", Academic Press, NY, 1976

[4] Thompson, H. and Stevenson, W.H. "Laser Velocimetry and Particle Sizing", Hemisphere Publishing Corporation, NY, 1979

[5] Bean, V.E. and Hall, J.M., "New Primary Standards for Air Speed Measurement at NIST", Proceeding of the 1999 NCSL Workshop and Symposium, Charlottle, NC.

[6] Dopheide, D., Taux, G. and Narjes, L. "Accurate Flow Rate Measurements by Means of Laser Doppler Anemometry", 3rd Conference of the IMEKO Technical Committee on Flow Measurements TC9, FLOMEKO '83, September 20 - 22, 1983, pp. 51-59

[7] Kurihara, N., Terao, Y. and Takamoto, M. "LDV Calibrator for the Air Speed Standard between 1.3 to 40 m/s", 5th International Symposium on Fluid Flow Measurement, Arlington, Virginia April 2002

[8] Park, J.T., Cutbirth, J.M. and Brewer, W.H. "Hydrodynamic Perfomance of the Large Cavitation Channel", 4th ASME_JSME Joint Fluids Engineering Conference, Honolulu, Hawaii, July 2003

[9] Taylor, B. N., and Kuyatt, C. E., Guidelines for Evaluating and Expressing the Uncertainty of NIST Measurement Results, NIST Technical Note 1297, 1994 Edition, National Institute of Standards and Technology, Gaithersburg, Maryland.

[10] International Organization for Standardization (ISO), "Guide to Expression of Uncertainty in Measurement, Geneva, Switz., 1993 edition.

[11] Coleman, H. W. and Steele, W. G., "Experimentation and Uncertainty Analysis for Engineers," 2nd ed., John Wiley and Sons, NY, 1999.

[12] ISO, "International Vocabulary of Basic and General Terms in Metrology, 2nd ed.," International Organization of Standardization, Geneva, Switzerland, 1993.

[13] Benedict, R.P., Fundamentals of Temperature, Pressure, and Flow Measurement, (John Wiley and Sons, New York, 1969), p. 245.

[14] Ower, E. and Pankhust, R.C. The Measurement of Air Flow, 4th ed. Pergamon Press, 1966

[15] Dryden, H., Murnaghan, F.D., and Bateman, H., Hydrodynamics, Dover Publication, Inc., 1956

[16] Jaeger, K. B. and Davis, R. S., A Primer for Mass Metrology, NBS Special Publication 700-1, November 1984, National Bureau of Standards, Gaithersburg, MD.

[17] Melnik, W.L. and Weske, J.R. Advances in Hot-wire Anemometry, Proceedings of the International Symposium on Hot Wire Anemometry, 1967

Appendix A: Sample Calibration Report

REPORT OF CALIBRATION

FOR

AIR SPEED INSTRUMENTATION
May 01, 2007
Shortridge Model ADM 870C Airdata Multimeter Serial Number M03327 with Airflow Technical Products Pitot-Static Tube Serial Number T12

submitted by

ABC Scientific
1234 ABC Drive
Any City, Any State xxxxx

(Purchase Order Number 1234-07 dated April 2, 2007)

The calibration of the instrument described above, was performed in the 1.5 m by 2.1 m rectangular test section of the NIST Dual Test Section Wind Tunnel. The instrument under test (IUT) was supported near the center of the tunnel in a manner that presented negligible interference with the flow (see Figure 1).

The air speed was measured by the NIST Laser Doppler Anemometer (LDA). The NIST LDA and its support were located about 0.5 m upstream of the anemometer under test so that the flow measured by the LDA was not perturbed by the presence of the instrument under test.

The temperature, pressure, and the relative humidity were measured in the test section of the wind tunnel during the test. Two calibration cycles were done separated by a shutdown. In each calibration cycle, the air speed was measured five times at each air speed set point. The output (V_{IUT}) from the instrument under test was gathered visually and recorded.

The results for the instrument presented in Table 1 and in Figure 2 were calculated using the means of the 10 measurements at each speed. Table 1 lists the air speed from the NIST LDA (V_{NIST}), the air speed from the instrument under test (V_{IUT}), the temperature, pressure, and relative humidity of the air at the wind tunnel test section, the air speed ratio (V_{IUT}/V_{NIST}), and the expanded uncertainty values for the air speed ratio The uncertainties of the instruments that measure temperature, pressure, and relative humidity values listed in the Table 1 are 1 K, 0.1 kPa, and 5 % respectively.

The air speed ratio, V_{IUT}/V_{NIST}, is plotted in Figure 2 with error bars that represent the expanded

uncertainty calculated as described below.

Figure 1. Instrument under test in NIST Wind Tunnel, viewed from upstream and the readout.

The expanded uncertainty of the calibration of the instrument under test, U, can be calculated by[1, 2]

$$U = k\sqrt{u_{V_{NIST}}^2 + u_{Acq}^2 + u_R^2}\,, \qquad (1)$$

where the quantity k is the coverage factor, taken to be 2.0 to convert the combined uncertainty (67 % confidence level) to the expanded uncertainty (95 % confidence level). The quantity

[1] B. N. Taylor and C. E. Kuyatt, *Guidelines for Evaluating and Expressing the Uncertainty of NIST Measurement Results*, NIST Technical Note 1297, National Institute of Standards and Technology, January 1993.

[2] Coleman, H. W. and Steele, W. G., *Experimentation and Uncertainty Analysis for Engineers*, 2nd ed., John Wiley and Sons, Inc., 1999.

$u_{V_{NIST}}$ is the standard uncertainty of the air speed measurements made with the LDA. The expanded uncertainty of the LDA is $\sqrt{(0.0036\ m/s)^2 + (0.0064\ V_{LDA})^2}$ and the standard uncertainty is half of the expanded uncertainty.[3]

Table 1. Shortridge Model ADM 870C Airdata Multimeter Serial Number M03327 with Airflow Technical Products Pitot-Static Tube Serial Number T12 in the NIST Wind Tunnel

NIST Air Speed (V_{LDA}) [m/s]	IUT Output (V_{IUT}) [m/s]	Tunnel Static Temperature [K]	Tunnel Static Pressure [kPa]	Tunnel Relative Humidity [%]	Airspeed Ratio V_{IUT}/V_{LDA}	Expanded Uncertainty [%]
0.279	0.292	297.9	99.9	59	1.045	7.44
0.411	0.424	297.6	99.9	62	1.030	4.09
0.641	0.652	297.4	99.9	64	1.017	1.66
0.837	0.849	297.4	99.9	65	1.014	1.87
0.976	0.986	297.2	99.9	68	1.010	1.54
1.557	1.569	296.5	99.9	69	1.008	0.96
1.988	2.002	296.8	99.9	69	1.007	0.78
3.129	3.146	296.6	99.9	69	1.006	0.72
4.056	4.081	295.9	99.9	72	1.006	0.65
5.910	5.946	296.3	99.9	69	1.006	0.67
8.052	8.107	297.2	99.8	65	1.007	0.63
10.20	10.27	297.0	99.8	65	1.007	0.64
12.09	12.17	296.7	99.8	65	1.007	0.65
14.01	14.11	296.7	99.8	65	1.007	0.64
16.11	16.23	297.1	99.8	64	1.008	0.69
18.05	18.20	297.5	99.8	62	1.008	0.65
20.10	20.30	297.8	99.8	61	1.010	0.70

[3] Yeh, T.T.and Hall,J.M., *Air Speed Calibration Service*, NIST Special Publication 250-79, National Institute of Standards and Technology, Gaithersburg, Maryland.

The quantity u_{Acq} is the standard uncertainty of the data acquisition system and instrumentation used to obtain the readings from the instrument under test. In this case, the uncertainty due to data acquisition is less than or equal to 0.1 % and can be considered negligible. To measure the reproducibility[4] of the test, u_R, the standard deviation of the air speed ratio at each of the nominal air speeds was used to calculate the relative standard uncertainty (the standard deviation divided by the mean and expressed as a percentage).

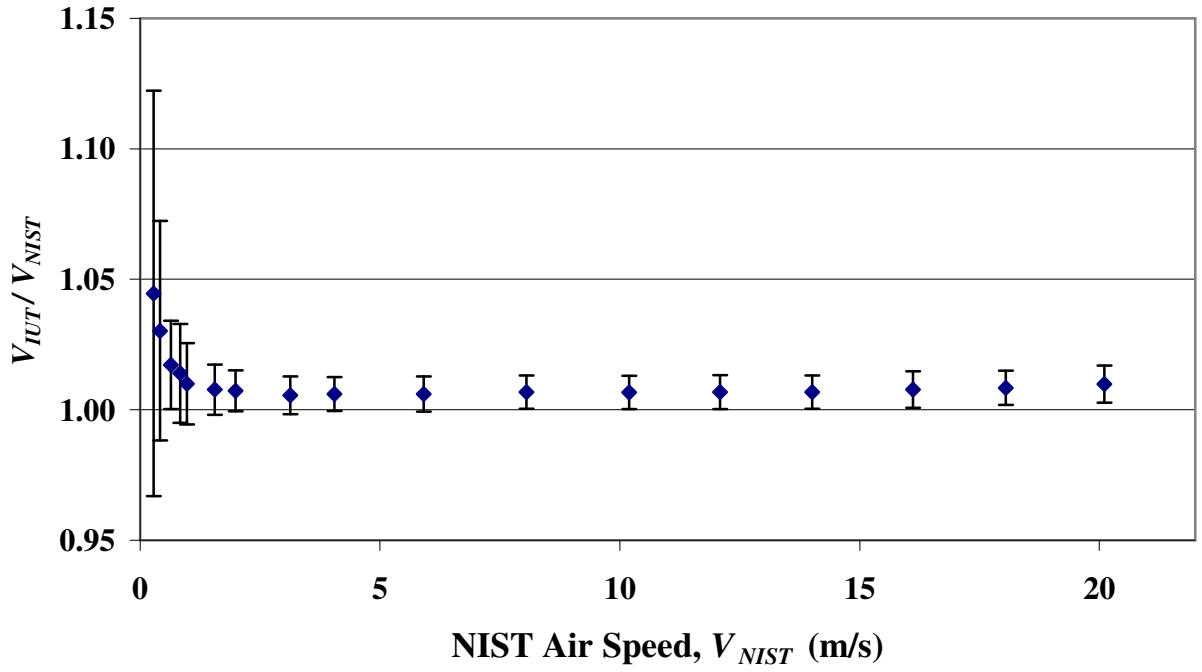

Figure 2. Graph of current and previous calibration results.

[4] Closeness of the agreement between the results of measurements of the same measurand carried out under changed conditions of measurement. Defined in the ISO, "International Vocabulary of Basic and General Terms in Metrology, 2nd ed.," International Organization of Standardization, Geneva, Switzerland, 1993. Reproducibility is herein defined as the closeness of agreement between measurements with the air speed changed and then returned to the same nominal value. Data collected on two different days are considered in this report.

For the Director,
National Institute of Standards and Technology

Fluid Metrology Group
Process Measurements Division
Chemical Science and Technology Laboratory